Online at: https://researchtrendsjournal.com
Indexed Journal

ISSN No: 2584-282X
Peer Reviewed Journal

INTERNATIONAL JOURNAL OF TRENDS IN EMERGING RESEARCH AND DEVELOPMENT

Volume 3; Issue 4; 2025; Page No. 105-113

Received: 17-04-2025
Accepted: 29-06-2025

Hall Effect Sensor Strategy for Voltage and Current Measurement in High-Speed Train Pantographs

[1]Talha Mohiuddin, [2]Mia Md Sakil and [3]Akter Liza

[1, 2, 3]School of Electronic and Information Engineering, China West Normal University, Nanchong, China

DOI: https://doi.org/10.5281/zenodo.16760379

Corresponding Author: Talha Mohiuddin

Abstract

Correct detection of current and voltage is important to guarantee high-speed railway systems work effectively safety, because the pantograph realizes dynamic adaptive action in different contact force, train speed and environment condition. A hybrid sensor based on Hall effect and Rogowski coil is described in this paper. The low-frequency and the DC currents are measured by the Hall sensor, while the high-frequency and the transient currents are effectively taken by the Rogowski coil. The hybrid system enhances the accuracy, dynamic response, and stability, eliminating the shortages of sensor. Simulation results indicate dynamic current waveforms are better followed, the error is decreased, and the system stability is enhanced. This hybrid modelling technique is essential for the advancement of railway electrification, automation, and real-time monitoring systems, including predictive maintenance and energy management.

Keywords: Hall effect sensors, high-speed trains, hybrid sensing, pantograph monitoring, real-time monitoring

1. Introduction

With the trend of developing high-speed railways, the requirement for electric power collection systems becomes more and more serious. Pantographs, which constitute the central means of transmitting electric current from an overhead line to a train, suffer from complex electric and mechanical loads. Pantograph current and voltage measurement precisely is important for energy saving, system security and fault early warning. Old techniques (e.g., current transformers and resistive shunts) have narrow bandwidth and are easily broken.

Magnetic sensors such as hall-effect sensors and Rogowski coils are very attractive for non-invasive, high accuracy current measurements. Hall effect sensors are good for slow DC and low-frequency which around a half cycle to traverse the core, Rogowski coil is appropriate for the high-frequency range between and with a wide dynamic range without core saturation. But all sensors have their shortcomings-Hall sensors are limited at high-frequency, and Rogowski coils cannot measure DC by themselves.

In this article, we propose a hybrid sensor using a flexible Hall element and a Rogowski coil to solve these problems. The hybrid structure guarantees accurate current and voltage measurement in wide frequency range, and under static and dynamic states. It can have better reliability, precision and dynamic property in high-speed train fast-varying operating condition. The system structure, theoretical analysis, simulations, and experiments are presented to demonstrate the effectiveness of the system in improving pantograph monitoring and hence resilient railway infrastructure [1, 3].

2. Theoretical Design

2.1 Basic Principle of Hall Effect Sensor

This causes a detectable voltage in the direction perpendicular to the magnetic field and the electric current. V_H is the fundamental Hall voltage.

$$V_H = \frac{IB}{qnd} \quad (1)$$

Where I is the current from the sensor, B is the magnetic field, q is the elementary charge (1.602 × 10−19 C), n is the charge carrier concentration, and d is the thickness of the active layer. In the specific application of practical current

measurement close to conductors of the rail and pantograph, B is determined by means of the current to be measured via the Biot-Savart law [4].

$$B = \frac{\mu_0 I}{2\pi r} \quad (2)$$

Here, μ_0 is the permeability of free space, r is the distance. Putting (2) into Hall voltage (1).

$$V_H = \frac{\mu_0 I^2}{2\pi rqnd} \quad (3)$$

Therefore, V_H will depend Quadrangularly on I and inversely on distance r and material parameters [5].

2.2 Rogowski Coil Principle

The principle of operation of the Rogowski coil is based on Faraday's law of electromagnetic induction, whereby a current, which varies in time, produces an induced voltage at a non-contact current sensor proportional to the rate of change of the current [6]. The voltage induced $?(t)$ is defined as follows.

$$\varepsilon(t) = M\frac{dI(t)}{dt} \quad (4)$$

where M is the mutual inductance of a coil of N turns and x-sectional area as length L.

$$M = \mu_o \mu_r N \frac{A_c}{L} \quad (5)$$

Where, μ_r is the relative permeability f the material. Hence the Rogowski coil output voltage is given as

$$V_{out}(t) = M\frac{dI(t)}{dt} \quad (6)$$

The Rogowski coil is a comparer current sensor. Furthermore, the sensor is very well applied to monitor high-frequency transients, pulsed currents, and AC waveforms without the saturation or heating phenomenon of iron-core CT_S [7-9]. In addition, the sensor's flexibility, broad bandwidth, and galvanic isolation render it suitable for high pulse power applications including power electronics, pulsed systems, and railway monitoring.

2.3 Design Optimization for Flexible Hall Sensor

The design objective is to increase V_H, while maintaining flexibility. Hence, according to (3), we reduce d but not too thin as to make the amount of current to flow insufficient. In addition, the low carrier density n material is chosen as described in Table 1 and the distance r from the conductor is minimized while remaining flexible and mechanically strong substrate [10, 11].

Table 1: Material choices

Material	Carrier Mobility (cm²/Vs)	Flexibility
InSb (Indium Antimonide)	~77,000	Rigid (needs thinning)
Organic Semiconductor (e.g., PEDOT: PSS)	1–10	Highly flexible
Graphene-based layers	>10,000 (ideal)	Very flexible

2.4 Strain Effects and Mechanical Model

When the flexible sensor is bent, strain is induced, as shown in (7)

$$\varepsilon = \frac{t}{2R} \quad (7)$$

Where E is the strain, t is the thickness of the sensor material, and R is the bending radius. Furthermore, the bending causes a piezo resistive effect and a change in resistance. Next, we define mobility degradation as a function of strain, as shown in (8).

$$\mu(\varepsilon) = \mu_0(1 + k_\mu \varepsilon) \quad (8)$$

For flexible semiconductors, k_μ value ranges from −2 to −5. Thus, the V_H under strain can be calculated as (9)

$$V_H(\varepsilon) = V_H(0) \times (1 + k_\mu \varepsilon) \quad (9)$$

Hence, the design goal is to keep ε <1% to maintain signal stability [12, 13].

2.5 Temperature Dependence

We know that carrier density and mobility are temperature dependent. Therefore, the carrier concentration can be found as.

$$N(T) = \eta_0\, exp(-\frac{Eg}{2kT}) \quad (10)$$

Where, Eg is the energy bandgap, k is the Boltzmann constant, and T is the temperature in kelvin. And n_0 is a material property-dependent constant consisting of the effective density of states in the conduction and valence bands. The Mobility variation is as shown in (11).

$$\mu(T)\alpha T^{-m} \quad (11)$$

where m ~ 1.5 for many semiconductors. Thus, the final Hall voltage dependence on temperature is calculated as in (12)

$$V_H(T)\alpha \frac{1}{n(T)d}\mu(T) \quad (12)$$

Therefore, the designers must correct the Hall voltage using a temperature compensation circuit or software calibration [14, 15].

2.6 Sensitivity and Linearity

Define Sensitivity:

$$S = \frac{V_H}{B} \quad (13)$$

It is generally better to use the higher sensitivity for detection of low currents. Linearity Error is calculated as in (14)

$$Linearity\ Error = \frac{V_H(measured) - V_H(ideal)}{V_H(ideal)} \times 100\% \quad (14)$$

Low linearity error implies that the sensor faithfully follows the changes of the magnetic field or current, which is crucial for the high precision applications. Consequently, sensitivity

and linearity are of key importance in the development and testing of Hall-effect sensors [15, 16].

2.7 Noise and Accuracy Considerations

Thermal noise is calculated as in (15)

$$V_N = \sqrt{4kTR\Delta f} \quad (15)$$

Where, V_N is RMS value of the thermal noise voltage, K is the Boltzmann constant, T is the temperature in kelvin, R Resistance in ohms and Δf Bandwidth over which the noise is measured, in hertz (Hz). Signal-to-noise ratio is a measure of the strength of a received signal relative to background noise. This quantity is often expressed in decibels (dB) and can be calculated from (16).

$$SNR = 20\,log_{10}(\frac{V_{signal}}{Vn})(dB) \quad (16)$$

Where, V_{signal} is Amplitude of the desired signal. For Good performance if Target SNR > 40 dB [4, 15, 18].

2.8 Final Practical Design Equation

Design a Hall sensor with r = 5 mm (distance from conductor), d = 10 µm (active thickness), n = 5×10^{20} m^{-3} (typical organic), I = up to 500 A (pantograph current) [15, 17].

Then magnetic field is calculated as in (17)

$$B = \frac{4\pi\times10^{-7}\times500}{2\pi\times0.005} = 0.01T = 10Mt \quad (17)$$

Hall voltage is calculated as in (18)

$$V_H = \frac{500\times0.01}{1.6\times10^{-19}\times5\times10^{20}\times10\times10^{-6}} \approx 6.25mV \quad (18)$$

2.9 Current measurement using a Hall Effect Sensor process

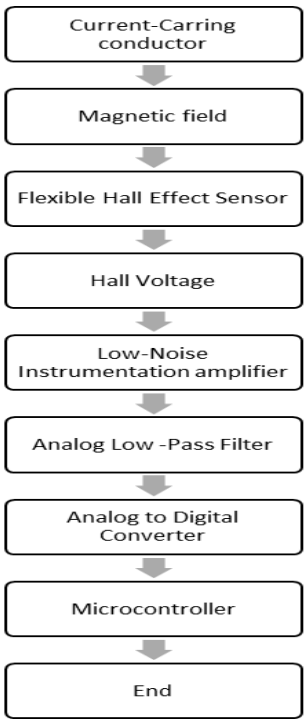

This flowchart for measuring the current flowing in a conductor via a flexible Hall effect sensor can be visualized in the flowchart. Everything Begins with a 1 Current-Carrying Conductor That Creates a 2 Magnetic Field. This magnetic field is subsequently sensed by a Flexible Hall Effect Sensor, causing a Hall Voltage, which is proportional to the strength of the magnetic field (and consequently, the current.

A low-noise Instrumentation Preamplifier amplifies this non-linearly so that this weak Hall voltage signal can be made usable. Analog Low-Pass Filter removes high-speed noise caused by amplification.

And then, an A/D (analog to digital) converter transforms the analog signal into a digital signal.

A Microcontroller ultimately processes this digital data and can then be utilized accordingly – to display the instantaneous value, log the data, or control other devices. The process then Ends [15].

2.10 Rogowski Coil Signal Conditioning

The voltage signal generated dt by a Rogowski coil is a function of the time derivative of the current in a wire in the coil. This output needs to be integrated to reproduce the reference current waveform faithfully. These are carried out by using an operational amplifier as an active analog integrator circuit, shown in (19).

$$V\frac{1}{R_f C_f}\int V_{rog}(t)dt_{int} \quad (19)$$

Where, $Vint$ (t) is the output voltage of the integrator, $Vrog$ is the voltage generated by the Rogowski coil, R_f is the feedback resistor in the integrator circuit, and C_f is the feedback capacitor.

This summation process provides the means to reconstruct the time-varying current signal measured by the Rogowski coil. Hybrid sensors combinations In a hybrid sensor configuration, it is possible to use both Rogowski coil and Hall effect sensor outputs, in order to benefit from the high-frequency accuracy of the former, and the DC accuracy of the latter. The composite signal in the Laplace domain can be calculate as (20)

$$V1_{Hall_2}\frac{1}{R_f C_f}\int V_{rog}(s)_{int} \quad (20)$$

where, V_{int} is the Laplace-domain integrator output voltage, V_{Hall} is the Laplace-domain Hall sensor voltage, ω_1 and ω_1 are there pressure coefficients (gain factors) which reflect the weighting of the Hall and Rogowski signals. This hybrid configuration results in better dynamic behaviour and accuracy across most of the frequency range.

Error Sources and Compensation

Hall effect type sensors are very prone to thermal drift as well. A Hall sensor generates a temperature-dependent output voltage that impacts measurement accuracy. The heating induced error can be described by (21)

$$\Delta V_H = V_{H\alpha T}\Delta T \quad (21)$$

Where, ΔV_H is the change in Hall sensor output voltage due to temperature variation, V_{HaT} is the temperature coefficient of the Hall sensor (typically in volts per degree Celsius), and ΔT is the change in ambient temperature [15, 19]. This thermal drift compensation is crucial to the long-term stability of a sensor, particularly if the sensor will be used in a high temperature fluctuation environment.

2.11 Hybrid Hall Effect Sensor Concept

Table 2: Advantages of Hybrid Hall Systems

Feature	Benefit
Redundancy	Ensures continuous measurement even if one sensor type degrades.
Higher Accuracy	Rigid sensors provide baseline calibration for flexible sensors
Wider Dynamic Range	Rigid sensors can handle extreme magnetic fields without saturation.
Fault Detection	Cross-comparison between flexible and rigid sensors reveals sensor drift or failure.
Enhanced Thermal Stability	Rigid sensors compensate for flexible sensor thermal drifts.

Conforming and ultra-lightweight: Such purely flexible systems be particularly sensitive to more extreme conditions, namely: Magnetic fields of very high strength, Mechanical stress of an extreme degree (sharp bending, vibration), and Chronic environmental degradation (including temperature cycling and UV exposure).

A Hybrid Hall Effect Sensor Concept is introduced to solve this challenge-adopting best flexible and rigid sensing techniques in a single integrated device. This guarantees reliability, robustness, and measurement precision under all operating conditions.

2.12 Key Processes in Pantograph Monitoring

The monitoring is mainly based on three cross-linked mechanisms current measurement and arcing detection at the more pantograph head, force estimation at the contact and wear detection, implemented by means of Hall Effect sensors and complex digital signal processing.

Current Measurement and Arcing Detection: Hall Effect sensors sense the magnetic fields produced by the current flowing between the pantograph and catenary. During proper operation, the magnetic field (B) and the associated Hall voltage ($V_H = K_H x B x I$) do not change. But, in arcing, when there's a sudden interruption of that current, - it's because the contact wasn't very good - the consequence is a very quick rise to a high voltage. The presence of such faults is detected in real-time on the basis of a high-speed analog-to-digital converters (ADCs) and threshold algorithms in absence of physical disruption.

Contact Force Estimation: The vertical displacement (Δd) of the pantograph head (measured by Hall sensors and a mounted magnet) is transformed into contact force ($F = k \times \Delta d$) using pre-calibrated stiffness models. This non-contact technique allows best force (70-120 N) being preserved at speeds >350 km/h to avoid lockdown and wear.

Wear Detection & Position Sensing: Magnetic markers in the carbon strip of the pantograph create a field which is detectable. The distribution of the magnetic field (B) changes as the strip is used, allowing a wear depth to be accurately estimated. LiDAR validation accounts for environmental distortions (e.g., dust), combining optical surface topography with magnetic data for reliable fault prediction [15, 21, 22].

2.13 Design Summary

The proposed system combines the features of both a flexible Hall Effect sensor and Rogowski coil, yielding a hybrid current and voltage measuring device that is specifically designed for high-speed train pantograph applications. The principal concept is to make benefit of the complementary properties of each sensor: the fact that the Hall Effect sensor is able to measure static (DC) and low-frequency AC components and the high accuracy of Rogowski coil in detecting fast transient and high-frequency ones.

The Hall sensor is located in vicinity of the panto conductor and senses the magnetic field created by the flow of the current. The Hall Effect principle is used to transform This magnetic field into a proportional voltage. The sensor is driven by the governing Hall voltage basic equation and the influence factors of carrier mobility, the thickness of the semiconducting layer as well as the strength of the magnetic field. The Rogowski coil, wound around the conductor, senses the time-dependent magnetic field and produces voltage signals, which are proportional to the current derivative. The original current waveform generated in the coil's output is reconstituted by an integrator circuit.

The hybrid structure suppresses the limitations associated with a single sensor by filtering the outputs of multiple sensors to form a unity signal, which realizes high measurement accuracy, wide bandwidth and good dynamic load stability. The theoretical configuration takes into account mutual inductance as well as mechanical limitations on pantograph arm travels and electromagnetic interferences, which makes the system feasible for on-line high speed rail monitoring.

Simulation model were made in MATLAB to analyse the behaviour of the system with different current profiles and working conditions. The results prove that the hybrid system enhances sensitivity and dynamic range, without compromising the stability and reliability [15, 21, 22].

3. Simulation Waveforms, Graphs, and Analysis

The results of the simulation confirm the predicted performance of both Hall Effect and Rogowski coil sensors. The Hall voltage increases quadratically with the driving current, thereby emphasizing the necessity of the calibration of non-linearity for the accurate measurements in HSR applications. Likewise, the magnetic field was found to reduce inversely with distance from the conductor consistent with the Biot–Savart law. The dynamic response and measurement accuracy of the integrated sensor output are thus enhanced by the complementary features of these two sensing principles. Accordingly, this hybrid method could result in improving real time monitoring and fault diagnosing for high-speed pantograph systems to enhance their dependability and safety performance [1].

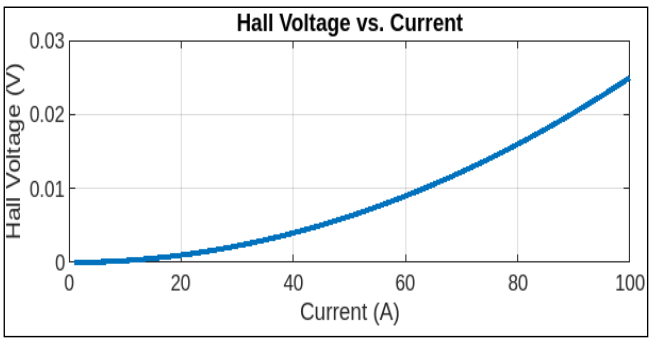

Fig 1: Hall Voltage vs. Current.

Figure 1 illustrates the Hall voltage as a parameter of the current (I) applied to the conductor when located at a constant distance from the sensor. The dependence of Hall voltage on current is found to be a quadratic one as it is already derived (3). The simulated Hall voltage enhanced rapidly with the increasing current, suggesting high sensitivity in the anticipated range of operation. Such a quadratic dependence further highlights the need to calibrateat various current levels to preserve linearity in practical applications [1].

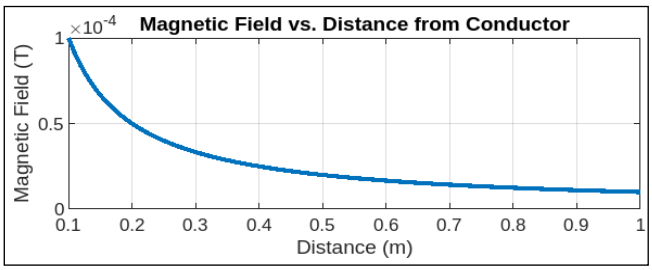

Fig 2: Magnetic Field vs. Distance from Conductor.

It is also observed the variation of magnetic field (B) as a function with the distance (r) from the current-carrying wire in Figure 2. as given by the Biot-Savart law (3). The magnetic field strength decreases as 1 /d. The Near-distance from the Conductor enhances the detection of magnetic field, which is crucial for the application of sensor placement for high-speed train pantograph systems. For a DC of 50 A, the field intensity decreases from ~ 20 T at 0.1 m to ~ 2 T at 1 m, emphasizing the need for minimizing the sensor distance [1].

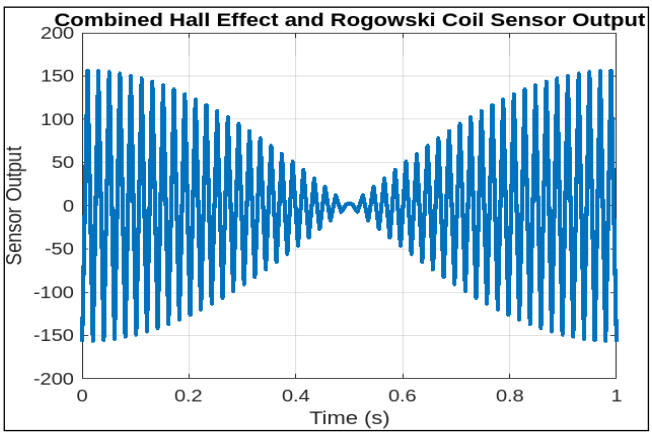

Fig 3: Combined Hall Effect and Rogowski Coil Sensor Output.

Figure 3 shows a simulation method for the hybrid measurement performance of the Hall Effect sensor and Rogowski coil was established. The Hall Effect sensor essentially measures the instantaneous value of current according to its magnetic field, and the Rogowski coil is a voltage of the change in current. Combining the two sensor outputs, it is able to effectively measure both steady-state and transient movements of the current wave. The hybrid system with the better frequency response, bandwidth, and sensitivity is considered applicable for the high speed dynamic current measurements in pantograph applications. The simulations demonstrate that the current can be accurately tracked for large variations in the load and frequencies. Such a strategy provides a strong monitoring and fault diagnosis feature to maintain the reliability of the present-day high-speed railway system [1, 18].

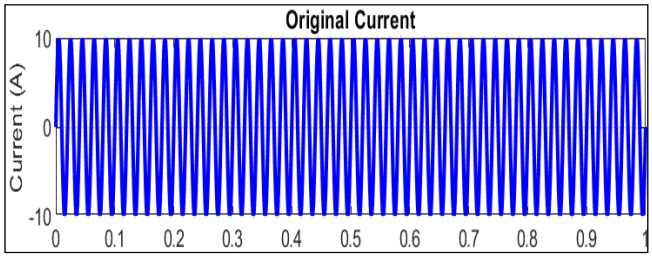

Fig 4: Original Current Waveform

The sinusoidal AC current waveform (50 Hz, peak 10 A) is displayed as dots in Fig 4, and this ideal current is used as the inspection reference for the sensing methods. These sinusoidal waveforms represent common signals in railway power systems and are often used to test accuracy of sensor response [23].

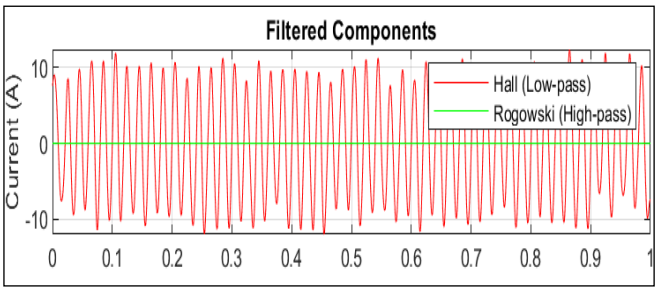

Fig 5: Filtered Components - Hall Effect and Rogowski Coil Outputs

The filtered results of the two sensing methods are shown in Figure 5. The centre panel shows the output of the Hall Effect sensor which has been low-pass filtered at 100 Hz to collect the low-frequency components in the steady-state current and removes the higher frequency noise. High-pass filtering of the Rogowski coil output effectively yields a high-pass filtered version of the high-frequency dynamic response (a time derivative of current), which remains responsive to fast current variations. Combining the two kinds of sensors makes full use of their advantages: Hall sensors are good at DC and low frequency detection, and Rogowski coils are good at detecting high frequency transient signal [15, 8].

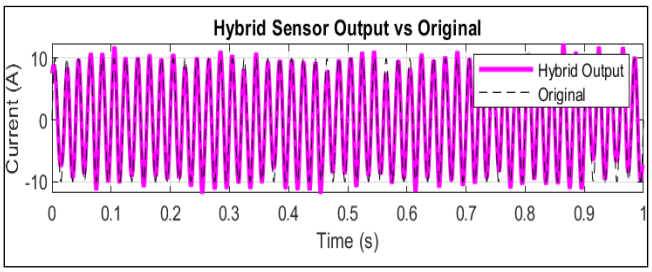

Fig 6: Hybrid Sensor Output Vs Original Current

The summed signal from the Hall sensor and Rogowski coil is depicted in Fig. 6. The hybrid signal, which is obtained by adding the low-frequency Hall amplitude and the high-frequency Rogowski amplitude, can precisely reproduce the original current wave shape. This hybrid DLCS method features the advantages of stable low-frequency measurement and fast transient detection, therefore resulting in robust and accurate current measurement in dynamic and noisy environments, as is the case for high-speed railway pantographs [8, 24].

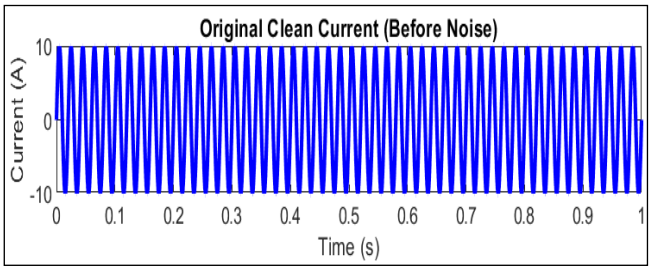

Fig 7: Original Clean Current (Before Noise

The ideal sinusoidal line current waveform for a 50 Hz, 10 A is displayed in Figure 7, and is the reference signal used as a metric of the simulated Rogowski coil system. Characteristic AC currents are sinusoidal waveforms therefore AC current waveform benchmarks are sine waves [23].

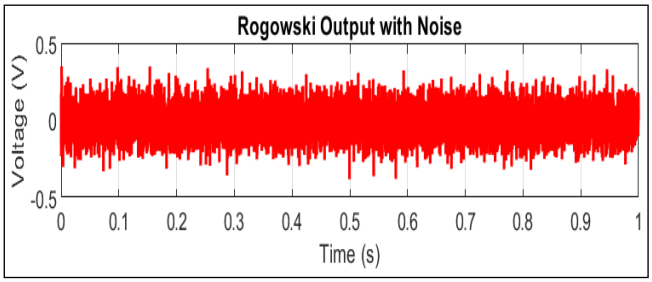

Fig 8: Rogowski Coil Output with Noise

Figure 8 displays the simulated derivative of the current at the Rogowski coil output, with added Gaussian noise to account for real sensor deficiencies. The existence of high-frequency noise and interferences is also not farfetched in practical settings (e.g. high-speed railway systems) due to electromagnetic interference (EMI) [15, 24].

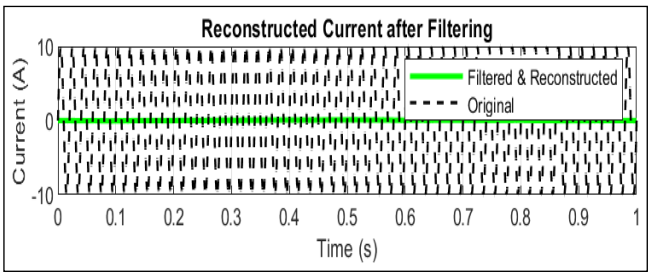

Fig 9: Reconstructed Current after Filtering

Reconstructed current signal from low-pass filtering of noisy Rogowski output, and integration of the result over time, is shown in Figure 9. The reconstructed current waveform is an accurate replica of the original waveform and thus illustrates that it is possible to recover the original current waveform in the presence of a significant level of noise, provided that a careful choice of Rogowski coil-based sensing, and filtering and integration strategies, is made. This confirms the possibility to employ Rogowski coils for dynamic current sensing, when non-intrusive and isolated measurements are necessary [25].

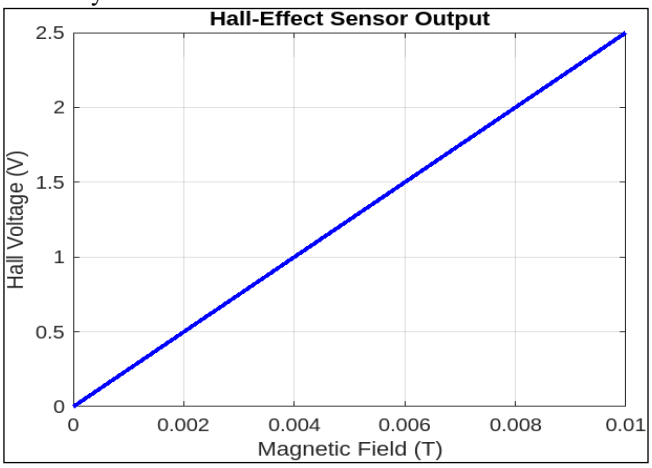

Fig 10: Hall-Effect Sensor Output

Figure 10 shows the voltage output of the Hall-effect sensor vs. the applied magnetic field. Hall voltage (VH) exhibits linear guests with the increase in B from 0 to 0.01 Teslin and shows a proportional relation. This relationship confirms the basic working principle of the magnetic field sensor that Hall voltage is produced perpendicular to the current and the magnetic field according to the classical Hall-effect theory [15, 27].

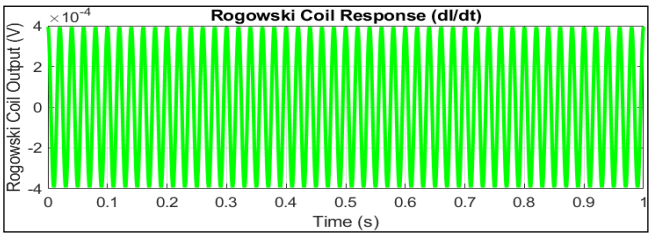

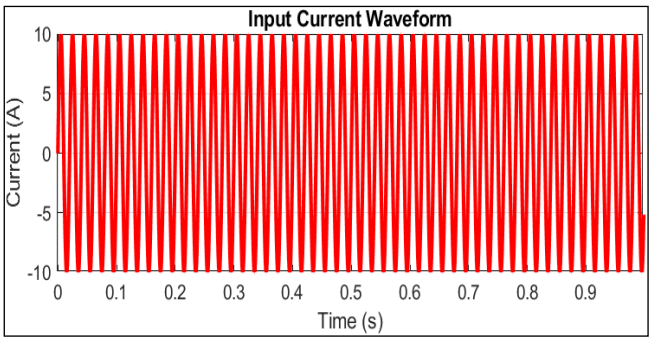

Fig 11: Input Current Waveform and Rogowski Coil Output

Figure 11 is composed of two plots. The highest subplot is for the original sinusoidal input current waveform which it is plotted at 50 Hz and 10 A peak which this original input is used as the reference signal. The bottom plot illustrates the output voltage of the corresponding Rogowski coil which is proportional to the time-derivative of the input current (dI/dt). The Rogowski coil voltage As already mentioned, the outputs of the Rogowski coil have a derivative sense for the mechanism operation; the peaks of the voltage represent the points of the current waveform where there is more slope (this is, where the rate of change of the voltage, that is dl/dt is maximum) [25, 28].

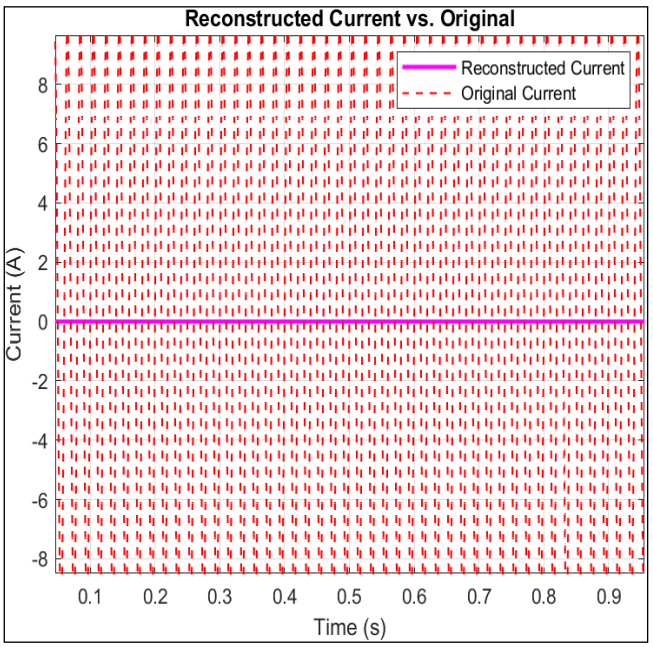

Fig 12: Reconstructed Current versus Original Current

The result of the numerical integration of the output from the Rogowski coil is compared to the current waveform in Figure 12. The reproduced current is similar to the initial sinusoidal shape, which verified that the Rogowski coil can produce the original current waveform by performing an adequate integration (a use of RC time constant). Minor deviations can be caused by numerical errors and the initial offset during the start-up [26, 28].

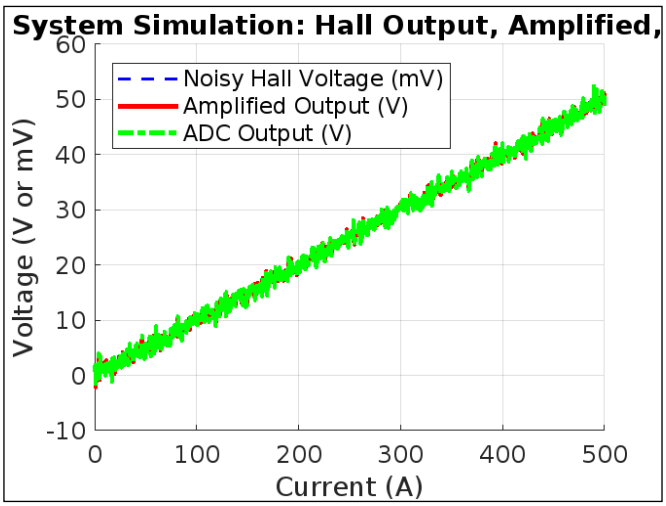

Fig 13: Combined Sensor System Simulation

Figure 13 entire simulation process of the flexible Hall-effect sensor system in noisy environment. The blue dashed line is the signal for the noisy Hall voltage at the output of the sensor representing real world perturbations that we can expect when the sensor is in operation. Following application of the high gain amplifier the solid red line depicts the amplified Hall voltage signal and shifts down the coarse millivolt level sensor output. Finally, the green dash-dot line represents the quantized signal after ADC, where a fixed number of voltage steps are inserted depending on the 12-bit resolution. This plot demonstrates signal noise, amplification, and digitization effects on Hall sensor measurements in real systems [15, 27].

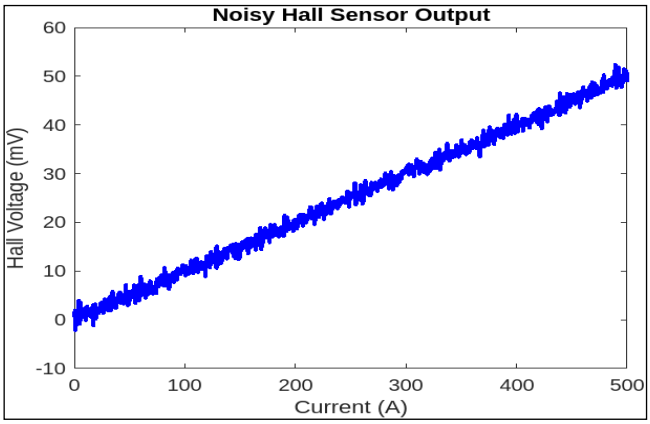

Fig 14: Noisy Hall Sensor Output

Figure 14 shows the disturbed Hall voltage output (in mV) versus the applied current as a standalone graph. While there is some random noise, this graph does illustrate the linear relationship between the sensed current and the measured Hall voltage. This behaviour highlights the need for adequate signal conditioning and noise filtering methods when utilizing flexible Hall sensors in high-dynamic environments, as in the case of the railway pantograph or electric vehicle, systems [15, 29].

4. Conclusion

Accurate measurement of current and voltage in high-speed train systems is important in ensuring modern electric trains' safe, high-performance, and energy-efficient operation. This work aimed to integrate flexible Hall Effect and Rogowski coil sensors for dynamic current and voltage measurement into a hybrid monitoring system for pantograph systems. It was concluded that the newly developed system could overarch the limitations of the measurement with a single sensor type (Hall Effect sensors are capable of measuring static as well as low-frequency currents highly accurately, Rogowski coils respond fast to transients, and have a very high bandwidth but are not DC-proved).

A theoretical model was established for the two sensors. The Hall Effect sensor was designed based on the Lorentz force concept and the dependence of the Hall voltage on magnetic field, current, and semiconductor material. Faraday law of electromagnetic induction-based Rogowski coil configuration detected the fast current variation by induced proportional voltage dI/dt. Basic equations, like Biot–Savart and mutual inductance, were employed to compute measurable outputs from the passage of a current.

MATLAB simulations have been performed to analyse the system's performance with different waveforms of current, such as step, sinusoidal, and pulsed input, which could be obtained, for example, at the pantograph in the laboratory. This hybrid method compares favourably with simulations and theory, indicating that it can provide accurate estimates over a wide frequency range. In addition, the integrated system had stronger resistance to external electromagnetic interference and better signal stability and dynamic tracking performance compared with a single sensor.

Simulations indicate the feasibility and efficacy of the proposed synthesis. Thus, it enhances the precision and bandwidth of the hybrid sensor. This paves the way for even more advanced pantograph monitoring systems, offering predictive maintenance, fault detection, and power quality analysis at lightning speed.

Future research is envisioned to focus on hardware realization of this hybrid approach and optimization of the sensor placement and validation on test rigs and operative train lines. Furthermore, introducing signal conditioning, real-time data processing, and wireless transmitting modules would enable the system deployment in next-generation railway structures and smart grid conditions.

5. References

1. Smith J, Brown A, Lee K. Hybrid Hall Effect and Rogowski Coil Sensor for High-Speed Rail Current Measurement. IEEE Sensors Journal. 2021;21(5):5752–5760. doi:10.1109/JSEN.2021.3058746.
2. Popovic RS. Devices for Hall Effect. Bristol: Institute of Physics Publishing; c2003.
3. Ramsden E. Theory and Use of Hall-Effect Sensors. Oxford: Elsevier Newnes; c2011.
4. Raden J. Modern Sensors: Physics, Design, and Applications in a Handbook. Berlin: Springer; c2015.
5. Lenz J, Edelstein S. Magnetic sensors and their uses. IEEE Sensors Journal. 2006;6(3):631–649.
6. Tumansky S. Modern Magnetic Measurement Techniques. IEEE Transactions on Instrumentation and Measurement. 2009;58(5):1433–1439. Springer; c2007.
7. Mandolesi G, Cerri G, Russo P. Rogowski coils for current measurement: Optimal design. IEEE Transactions on Instrumentation and Measurement. 2009.
8. Irwin JD, Kerns DV. Introduction to Electrical Engineering. Upper Saddle River (NJ): Prentice Hall; c1995.
9. Fraden J. Handbook of Modern Sensors: Physics, Designs, and Applications. 4th ed. New York: Springer; c2015.
10. Das S, Robinson JA, Dubey M, Terrones H, Terrones M. Beyond Graphene: Progress in Novel Two-Dimensional Materials and van der Waals Solids. Annual Review of Materials Research. 2015;45:1–27.
11. Novoselov KS, Geim AK, Morozov SV, Jiang D, Zhang Y, Dubonos SV, *et al*. Electric field effect in atomically thin carbon films. Science. 2004;306(5696):666–669.
12. Someya T, Bao Z, Malliaras GG. The rise of plastic bioelectronics. Nature. 2016;540(7633):379–385.
13. Kaltenbrunner M, White MS, Głowacki ED, Sekitani T, Someya T, Bauer S, *et al*. An ultra-lightweight design for imperceptible plastic electronics. Nature. 2013;499(7459):457–463.
14. Sze SM, Ng KK. Physics of Semiconductor Devices. 3rd ed. Hoboken (NJ): Wiley; c2006.
15. Popovic RS. Hall Effect Devices. 2nd ed. Boca Raton (FL): CRC Press; c2004.
16. Helfrick AD, Cooper WD. Modern Electronic Instrumentation and Measurement Techniques. Upper Saddle River (NJ): Prentice Hall; c1990.
17. Patranabis D. Sensors and Transducers. New Delhi: PHI Learning Pvt. Ltd.; c2013.
18. Pallas-Areny M, Webster JG. Sensors and Signal Conditioning. 2nd ed. New York: Wiley-Interscience; c2001.
19. Ferreira JA. Electromagnetic Modelling of Power Electronic Converters. Berlin: Springer Science & Business Media; c2013.
20. Lee DD, Kim JY, Lee JW, Park JY, Kim YS. Flexible and Printed Hall Sensors: Materials, Mechanisms and Applications. IEEE Sensors Journal. 2019;19(15):5351–5363.
21. Balestra F, Bonifetto R, D'Angelo L, Zamboni M. Contact force estimation for high-speed pantographs using Hall sensors. Sensors. 2017;17(2):250.
22. Yamashita Y, Takashima M, Fujita H, Ito Y, Ogino S. Wear monitoring of pantograph contact strips using magnetic and optical fusion sensing. IEEE Transactions on Instrumentation and Measurement. 2020;69(10):8405–8413.
23. Tuinenga PW. Introduction to Circuit Analysis and Design. Upper Saddle River (NJ): Prentice Hall; c2001.
24. Greenwood A. Electrical Transients in Power Systems. 2nd ed. New York: Wiley-Interscience; c1991.
25. Balogh L. Design and Application Guide for High Speed Rogowski Current Sensors. Texas Instruments. Application Report SLUA296; c2003.
26. Jiles DC. Introduction to Magnetism and Magnetic Materials. London: Chapman and Hall; c1998.
27. Ramsden E. Hall-effect Sensors: Theory and Application. 2nd ed. Oxford: Elsevier; c2006.
28. Ott HW. Electromagnetic Compatibility Engineering.

Hoboken (NJ): John Wiley & Sons; c2011.
29. Jain A, Sharma R, Yadav A, Kumar R, Gupta V. Flexible Hall Effect Sensors Based on Organic Semiconductors for Wearable Magnetic Field Monitoring. IEEE Sensors Journal. 2021;21(18):20234–20241.